Effects of antenna element structure on element properties and array pattern of a planar phased array

Shoichiro Fukao Toru Sato Hiroshi Hojo Iwane Kimura and Susumu Kato

Reprinted from
RADIO SCIENCE
Volume 21 Number 1 January/February 1986

Radio Science, Volume 21, Number 1, Pages 56–64, January–February 1986

Effects of antenna element structure on element properties and array pattern of a planar phased array

Shoichiro Fukao[1,2], *Toru Sato*[2], *Hiroshi Hojo*[1,3], *Iwane Kimura*[1], *and Susumu Kato*[2]

(Received January 23, 1985; revised July 23, 1985; accepted August 8, 1985.)

A numerical consideration is performed on degradation of element properties and array patterns of a planar phased array owing to the effects of antenna element structure. By using a crossed 3-subelement Yagi antenna specially designed for the VHF-band MST radar in Japan (the MU radar) as a model of antenna element. the following two subjects are investigated: (1) mutual coupling effects induced by deviation of the intersecting point of a pair of crossed subelements from each subelement center, and (2) effects of vertical current which flows on the mast supporting the antenna subelements. It is concluded that neither of them provide significant degradation of either element properties or array patterns. Although this conclusion is derived for specific phased arrays composed of specific antenna elements, it will be essentially valid for ordinary planar phased arrays composed of dipoles or Yagi antennas.

1. INTRODUCTION

Large phased arrays with an aperture of 10^4 to 10^5 m^2 are indispensable to the VHF Doppler radars known by the name of MST (mesosphere-stratosphere-troposphere) radar. The MST radars which incorporate high power transmitter(s) and sensitive receiver are capable of observing the various dynamical processes in the middle atmosphere (altitude range: 10–100 km). We have not restated the wide-ranging results obtained to date; readers are referred to the review papers by *Balsley and Gage* [1980, 1982] and *Larsen and Röttger* [1982].

The same type of radar was completed at Shigaraki, Japan (34.85°N, 136.10°E), by the Radio Atmospheric Science Center of Kyoto University in November 1985 [*Fukao et al.*, 1980; *Kato et al.*, 1984]. This radar has been named MU radar after the middle and upper atmospheres that are principally investigated with this system. The operational frequency is 46.5 MHz (wavelength: $\lambda = 6.45$ m), and the peak and average radiation powers are 1 MW and 50 kW, respectively.

The antenna arrays of the individual MST radars have various shapes, and are composed of a number of elements such as dipoles, coaxial collinear antennas or Yagis. The MU radar antenna is a circular phased array composed of 475 crossed 3-subelement Yagi antennas, which are arranged on equilateral triangular grids [*Kato et al.*, 1984]. The MU radar cannot fully scan the antenna beam, but its beam scanning capability is limited to within 30° from the zenith. The fundamental radiation properties including the mutual coupling effects were investigated elsewhere with the aid of an infinite array approximation [*Hojo et al.*, 1981].

In this paper, two remaining subjects concerned with the antenna element structure are considered quantitatively. Neither of them are conceivably the primary factor affecting the radiation properties, but still each of them seems a matter worthy to be considered, since they have been left uninvestigated due to the complexity in designing planar phased arrays. Although a specific crossed 3-subelement Yagi antenna used for the MU radar is employed as the model of antenna element, the present investigation will be essentially valid for ordinary antenna elements composed of dipole subelements.

2. SUBJECTS AND METHOD OF ANALYSIS

The antenna element structure used here is shown in Figure 1. As mentioned above, 475 antenna elements of this structure are installed for the MU radar antenna. The antenna mast which supports 3 pairs of crossed subelements intersects every subelement at right angles at their subelement centers. However, the two subelements do not intersect at their own centers, but the point of intersection deviates from the

[1]Department of Electrical Engineering, Kyoto University, Yoshida, Japan.
[2]Radio Atmospheric Science Center, Kyoto University, Uji, Japan.
[3]Now at NTT Electrical Communications Laboratories, Kanagawa, Japan.

Paper number 5S0648.
0048-6604/86/005S-0648$08.00

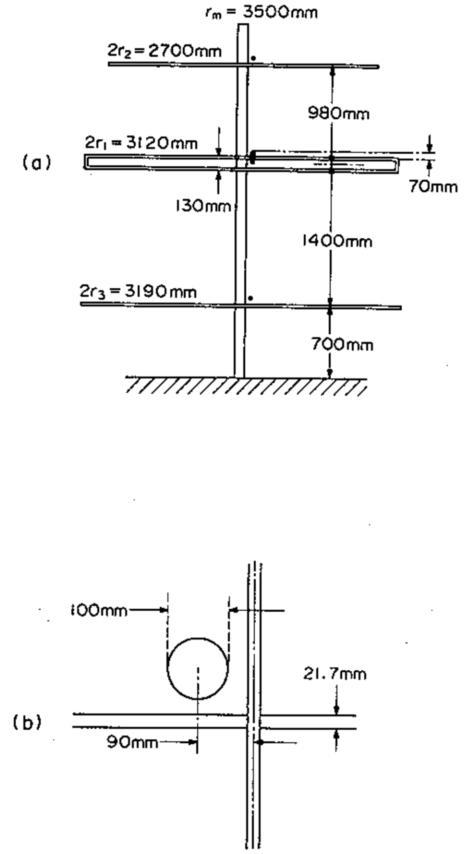

Fig. 1. (*a*) Front view of the crossed 3-subelement Yagi antenna used for the MU radar antenna; $2r_i (i = 1, 2, 3)$ is subelement length and r_m is height of the antenna mast. Height difference between a pair of crossed subelements is 70 mm. (*b*) Top view of the same antenna illustrated only in the vicinity of the mast.

centers by a distance of the order of the mast radius (see Figure 1, where the deviation is 90 mm). This results in mutual coupling between the two subelements. Therefore, the effect due to deviation of the point of intersection from each subelement center is investigated first.

Each mast, generally made of commercially available iron in order to obtain a sufficient strength, allows currents to flow vertically. As mentioned above, since the mast intersects each subelement at right angles at each subelement center, the mast provides no effect on the element properties in the case that a single Yagi antenna is situated in an infinite free space. But within an array the mast mutually couples with the subelements of other antenna elements, that causes degradation of both element properties and array pattern. This effect due to the current flowing on the masts is studied later.

We investigate the first subject for two array models with elements arranged in the same periodic way with the same spacing; one is an infinite array model and the other is a finite array model. Due to the computer memory size limitation, the number of antenna elements that can be analyzed for the finite array model is limited to approximately 70. Therefore, the finite array model is assumed to be a hexagonal one with 61 elements arranged as shown in Figure 2, where consecutive numbers represent the element positions. The main part of the MU radar antenna consists of 19 hexagonal subarrays, each of which is composed of 19 Yagi antennas shown in Figure 1 [*Kato et al.*, 1984]. As is also done in the MU radar antenna, the antenna elements are periodically arranged on equilateral triangular grids with element spacing of 0.7λ. This element arrangement does not form grating lobes at beam position within 40° from the zenith.

The current is determined by solving the circuit equation with the aid of improved circuit theory (ICT) [*Inagaki*, 1969]. The current is assumed by a linear combination of the following two functions for the radiator:

$$\left.\begin{aligned} I^1 &= I_0^1 \sin k(r_1 - |x|) \\ I^2 &= I_0^2\{1 - \cos k(r_1 - |x|)\} \end{aligned}\right\} \quad |x| \le r_1 \qquad (1)$$

and by the single function for both director and reflector:

$$I^3 = I_0^3(\cos kx - \cos kr_i) \qquad |x| \le r_i \ (i = 2, 3) \qquad (2)$$

where $k(=2\pi/\lambda)$ is the wave number and $2r_i$ $(i = 1, 2, 3)$ is subelement length.

The radiator for the MU radar antenna element is folded, and this effect is taken into account by using the geometrical mean distance of the cross section of the folded element as its effective radius. All elements

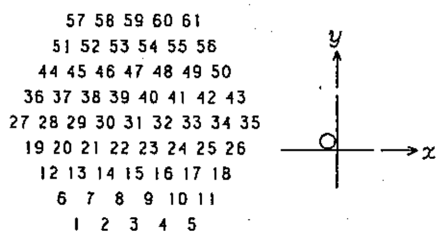

Fig. 2. (left) Hexagonal array composed of 61 Yagi antennas which are arranged on equilateral triangular grids with element spacing of 0.7λ (λ is wavelength). Consecutive numbers represent the element positions. (right) Top view of a Yagi antenna and the coordinate system.

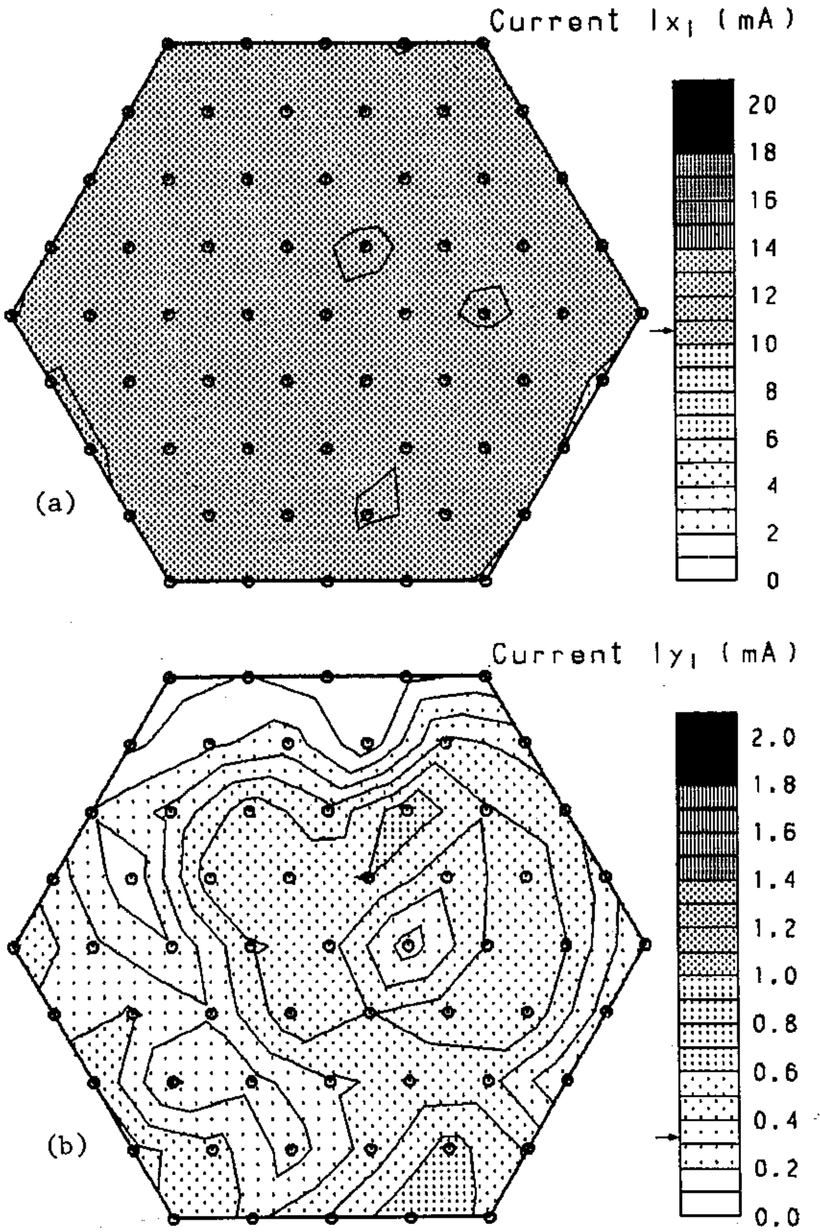

Fig. 3. Radiator currents of (*a*) the excited (*x*-aligned) subelements (Ix_1) and (*b*) the orthogonal (*y*-aligned) subelements (Iy_1) inferred with the orthogonal subelements included. The maximum currents are shown in a form of contour map for the case that the antenna beam is directed 30° off from the zenith in the *D* plane. Small circles indicate the element positions. The arrows placed on the counter scales on the right-hand side of each map indicate the values for the infinite array.

are assumed to be separately excited by an identical constant unit voltage with an internal serial impedance of 50 Ω, as is the case with the MU radar antenna. The ground plane is assumed to be a perfect conductor unless otherwise mentioned. Further details of the method of analysis are described elsewhere [*Fukao et al.*, this issue].

3. RESULTS

3.1. *Effects of deviation of subelement intersecting points from their centers*

It is assumed that only the *x*-aligned elements are excited, while the orthogonal elements are terminated

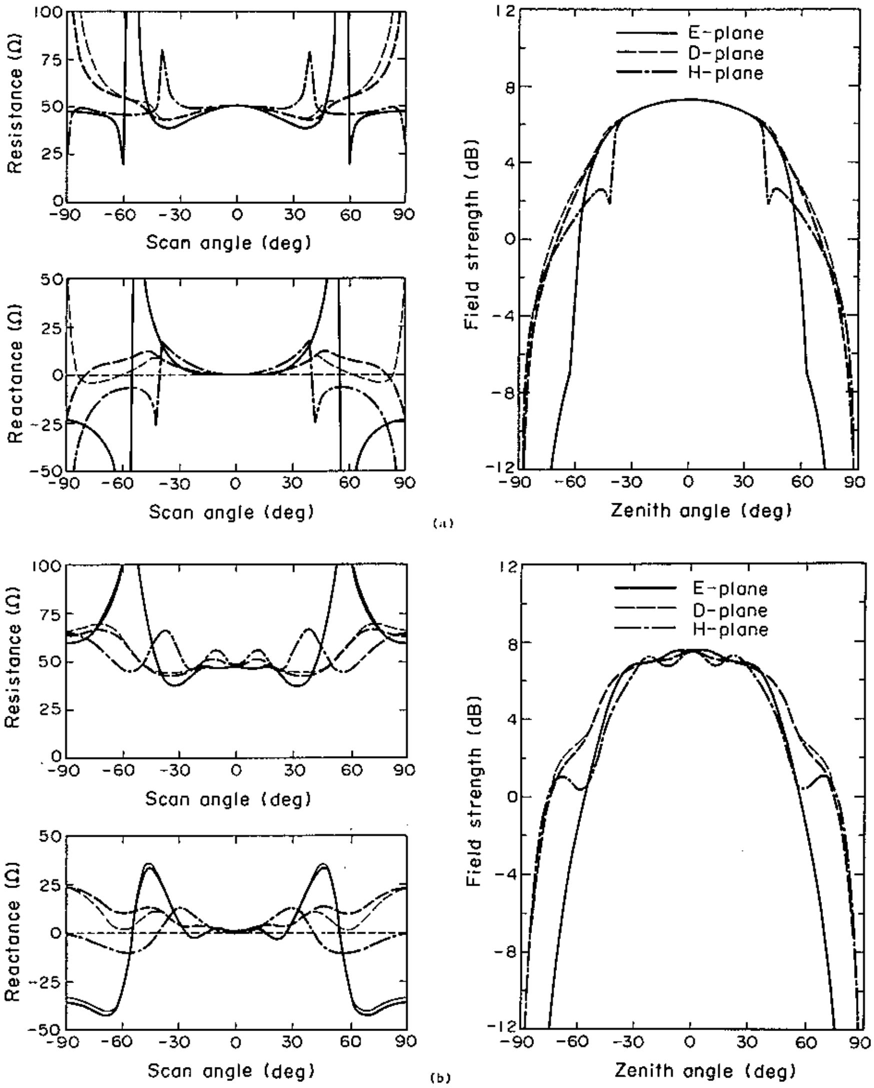

Fig. 4. Comparison of element properties between the cases with (thick lines) and without (thin lines) the orthogonal subelements included. The element properties are calculated for (*a*) the infinite array element and (*b*) the 31st (center) element of the finite array depicted in Figure 2. Active resistance and reactance components versus beam scan angle are shown in the top and bottom left, respectively, while the array element pattern versus zenith angle which is normalized to the radiation field of an isotropic antenna is given in the right. Solid and broken lines and chain indicate the properties in the *E*, *D* and *H* plane, respectively.

by the feed line impedance of 50 Ω. The mutual coupling with antenna masts is for now not taken into consideration.

The maximum values of radiator current on the excited (x-aligned) and the orthogonal (y-aligned) subelements are given in the form of a contour map in Figure 3. The antenna beam is directed 30° from the zenith (the maximum beam scan angle of the MU radar) in the D plane (diagonal: 45° with respect to the x axis). The mutual coupling between the two subelements is expected to be most significant at this beam direction. Each element position is indicated by a small circle. It should be noted that the current distribution is meaningful only at the element positions where the current is localized. Magnitudes of the same current components obtained for the infinite array model are indicated by the arrows placed on the contour scales on the right-hand side of each map. This figure illustrates that the currents induced on the orthogonal subelements are generally smaller

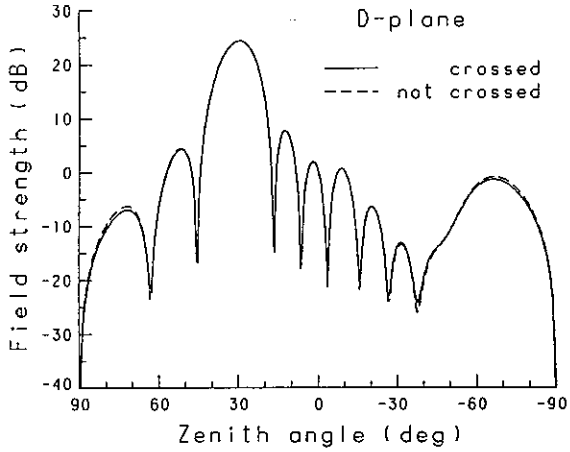

Fig. 5. Comparison of array pattern between the cases with the orthogonal subelements (solid line) and without them (dashed line). The abscissa is the zenith angle, while the ordinate is the electric field intensity over the radiation field of an isotropic antenna. The antenna beam is scanned by 30° off from the zenith in the *D* plane.

than 1/30 those on the excited subelements in both the finite and infinite arrays.

The element properties inferred with and without the orthogonal subelements included are compared in Figure 4. They are shown for both the infinite array element and the 31st (center) element of the finite array of Figure 2. Active resistance and reactance components are shown versus beam scan angle, and an array element pattern, which is normalized to the radiation field of an isotropic antenna matched to the feed line, is given against the zenith angle. The contribution from the orthogonal subelements is most significant in the *D* plane, of the order of 5–10 Ω, especially, at large beam scan angles. But any noticeable effect does not appear at beam scan angles within 30° (or inside the scan range of the MU radar antenna). Virtually no difference is perceived between the infinite and finite arrays in the way of contribution from the orthogonal subelements to the element properties.

Degradation of the array pattern is found negligible in Figure 5, by comparing the difference between the array patterns obtained with and without the contribution from the orthogonal subelements included. The pattern degradation is also examined for different values of the deviation. There appears no change from the pattern acquired without orthogonal subelements except for a 5–10 dB degradation at elevation angles less than 20° even for deviation as large as 270 mm. This suggests that random errors in collocating the antenna subelements (if small) affect only slightly the overall performance of the antenna.

3.2. *Effects of vertical mast current*

An antenna mast on which vertical current is induced works as a vertical dipole antenna. Here, the current distribution induced on each antenna mast is assumed in the form of (1). Since the current distribution is expected to vary with condition of the ground plane, the two extremely different cases depicted in Figure 6 are considered.

In case (A), the ground plane is assumed a perfect conductor, on which each antenna mast is earthed. A mast is regarded as a dipole antenna with a double length of the mast. In case (B), the antenna masts are not earthed on the ground plane which is assumed as a perfect conductor. Each mast works as a pair of dipoles aligned adjacently to each other.

First, the spatial current variation calculated for case (A) is represented in Figure 7. The beam is directed 30° from the zenith in the *E* plane where the vertical current is found to be most significant. Contour maps of spatial current variations shown in 7*a*, 7*b* and 7*c* correspond to the current flowing on excited (x-aligned) subelements, subelements orthogonal to the excited ones (y-aligned subelements), and antenna masts, respectively. This figure shows that amplitude of the vertical current induced on the antenna masts is generally on the order of 1/10 that of the current on excited subelements.

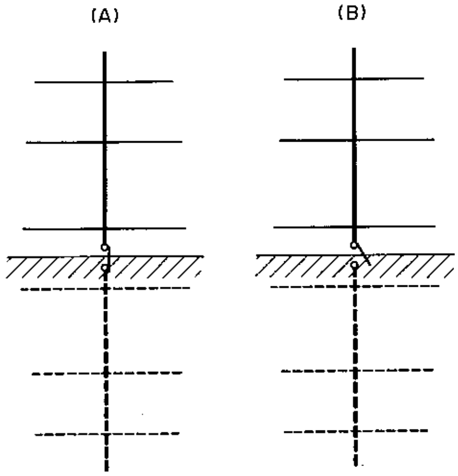

Fig. 6. Antenna mast and ground plane. (A) Antenna mast is earthed on a perfectly conducting ground, and (B) the ground plane is a perfect conductor, but the antenna mast is not earthed on it.

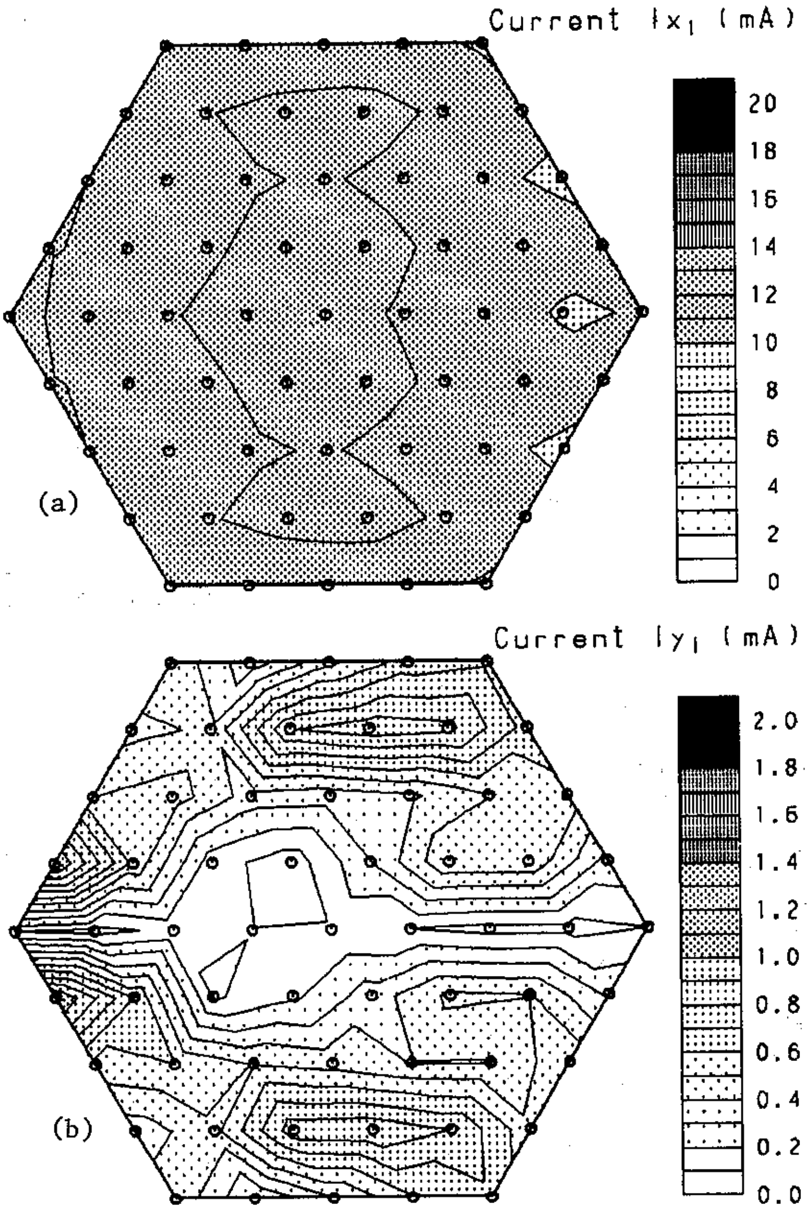

Fig. 7. Spatial current variations for case (A) in Figure 6. Current amplitudes on excited subelements (Ix_1), subelements orthogonal to the excited ones (Iy_1) and antenna masts (Ip) are depicted in 7*a*, 7*b* and 7*c*, respectively.

Figure 8 compares the array patterns calculated with and without the mast effects included. There is no appreciable difference between the two, except that the pattern nulls in the horizontal direction are raised to a level of about −30 dB. In Figure 9, a comparison is made between the element properties calculated with and without the antenna masts for the 29th element, on which the maximum vertical current is induced. The two element properties provide no appreciable difference within the beam scan range of 30° from the zenith, and the element pattern in the *E* plane differs only by 1 dB near zenith angle of 40°–50°. Thus, the mast effect can be concluded to be quite small in case (A) in Figure 6.

The spatial variation of mast current and array pattern obtained for case (B) in Figure 6 are shown

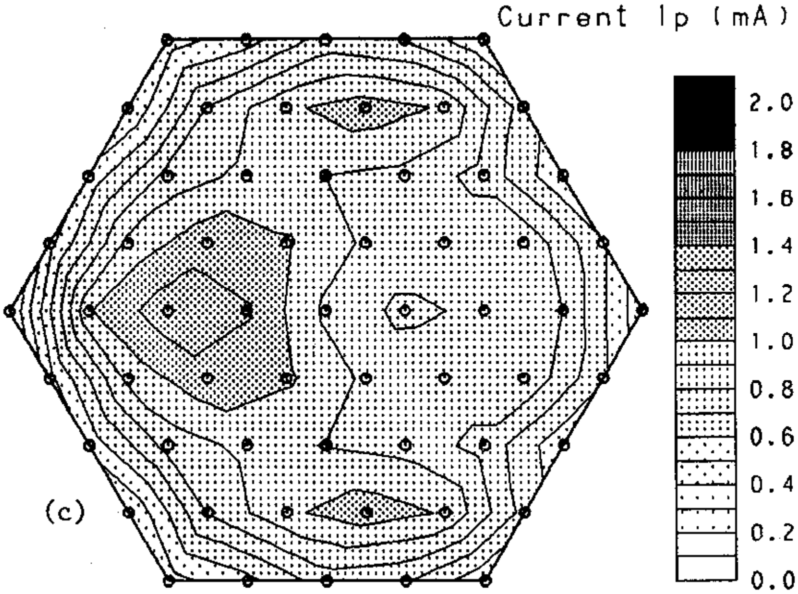

Fig. 7. (continued)

in Figure 10. The antenna beam is also directed 30° from the zenith in the E plane. A larger mast current flows in case (B) than in case (A), with a maximum amplitude of about 1/6 of that which is induced on the excited subelements. Hence, degradation of array patten due to the mast current is larger in case (B), but still it is no more than raising slightly the field strength at nulls in the array pattern at very low elevation angles. Very little difference of the element properties is also observed in the same calculation

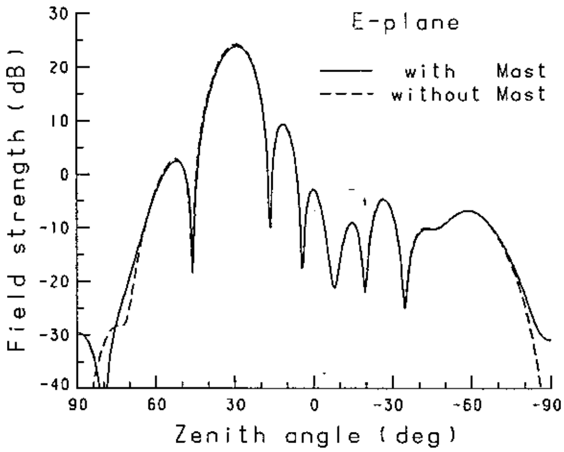

Fig. 8. Similar to Figure 5 except for comparison of array pattern between the cases with antenna masts (solid line) and without them (dashed line) for case (A) in Figure 6.

performed by changing the antenna mast height from $r_m - 200$ mm to $r_m + 200$ mm. Thus, though neither case (A) nor (B) seems to represent the real condition of the ground plane, the investigation on these two extreme cases indicates that the mast effect results in very little degradation of the array pattern.

4. CONCLUSIONS

Two factors that are expected to affect element properties and array pattern, though not primarily, are numerically investigated for a specific antenna element of the crossed 3-subelement Yagi antenna that is in actual use in the MU radar antenna. Main results obtained are as follows.

1. Effects of deviation of subelement intersecting point from their centers: The contribution of the orthogonal subelements to element properties is most significant in the D plane, but any noticeable change from the element properties obtained without the orthogonal subelements does not appear inside the scan range. Degradation of array pattern is also found negligible.

2. Effects of vertical mast current: A fairly large mast current flows in the case where each antenna mast is not earthed on a perfectly conducting ground plane. Amplitude of the maximum mast current is about 1/6 that on the excited subelements, but the degradation of array pattern is so small that only

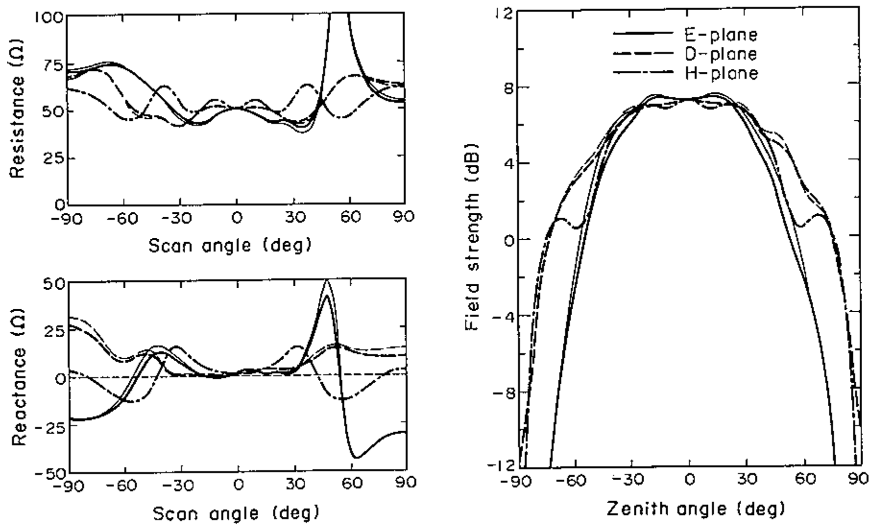

Fig. 9. Similar to Figure 4 except that comparison is made for the 29th element between the cases with (thick lines) and without (thin lines) antenna mast for case (A) in Figure 6.

field strength of pattern nulls at low elevation angles is slightly raised.

Thus, it is concluded that neither of the above two factors provide any serious degradation to both element properties and array pattern. The radiation properties of the MST radar phased arrays designed without these factors included will be altered very little if designed taking them into account. Also, random errors in collocating the antenna subelements, as long as they are not too large, affect only very slightly the overall performance of the array antenna. These conclusions derived for a specific element of crossed 3-subelement Yagi antenna will be essentially valid for ordinary planar phased arrays composed of dipoles of Yagi antennas with a limited scanning capability.

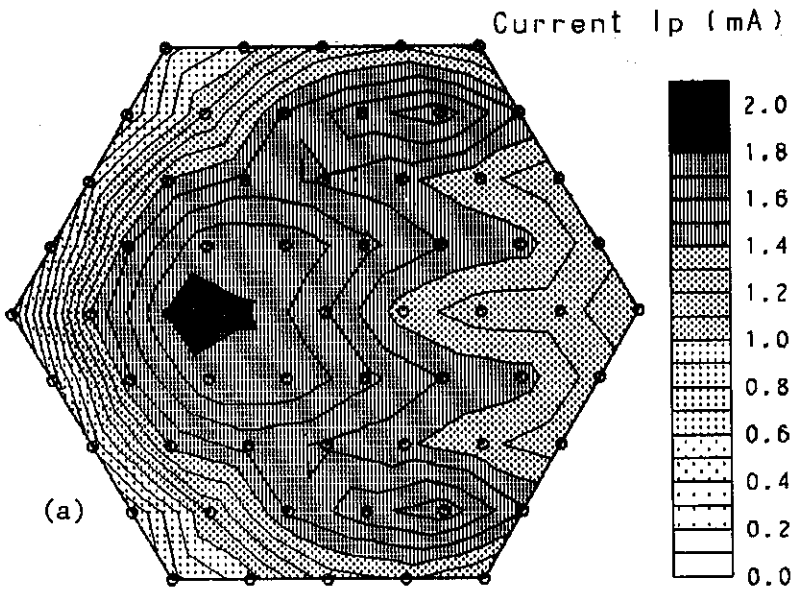

Fig. 10. (*a*) Spatial variation of mast current and (*b*) array pattern for case (B) in Figure 6. Array patterns with and without mast effects are represented by solid and dashed lines, respectively.

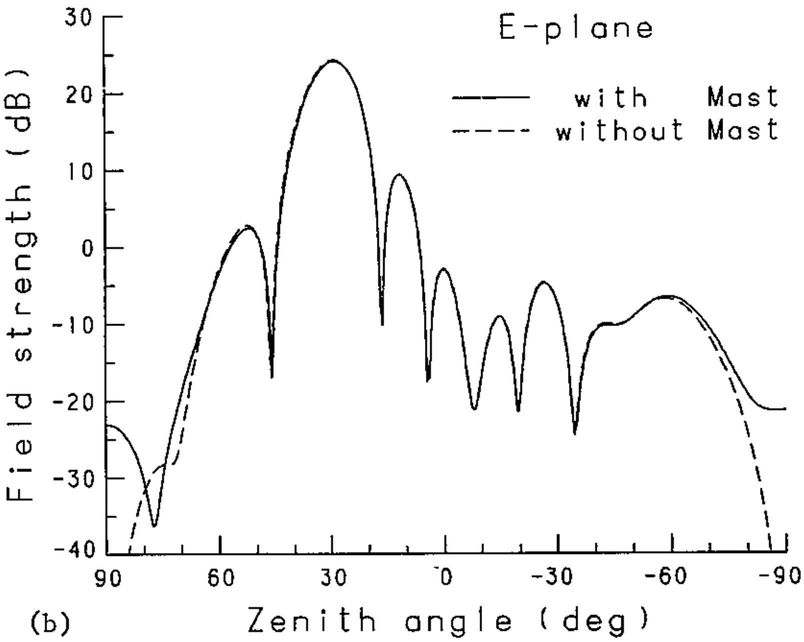

(b)

Fig. 10. (continued)

Acknowledgments. The authors thank S. Tokumaru, Keio University, for stimulating discussions. All computations were performed by FACOM-M382 at the Data Processing Center of Kyoto University.

REFERENCES

Balsley, B. B., and K. S. Gage, The MST radar technique: Potential for middle atmospheric studies, *Pure Appl. Geophys., 118*, 452–493, 1980.

Balsley, B. B., and K. S. Gage, On the use of radars for operational wind profiling, *Bull. Am. Meteorol. Soc., 63*, 1009–1018, 1982.

Fukao, S., S. Kato, T. Aso, M. Sasada, and T. Makihira, Middle and upper atmosphere radar (MUR) under design in Japan, *Radio Sci., 15*, 225–231, 1980.

Fukao, S., T. Sato, H. Hojo, I. Kimura, and S. Kato, A numerical consideration on edge effect of planar dipole phased arrays, *Radio Sci.*, this issue.

Hojo, H., T. Sato, S. Fukao, I. Kimura, and S. Tokumaru, Radiation characteristics of the MU radar phased array composed of crossed Yagi antenna elements (in Japanese), *Tech. Rep. IECE Jpn, AP81-52*, 49–56, 1981.

Inagaki, N., An improved circuit theory of a multielement antenna, *IEEE Trans. Antennas Propag., AP-17*, 120–124, 1969.

Kato, S., T. Ogawa, T. Tsuda, T. Sato, I. Kimura, and S. Fukao, The MU radar: First results using a partial system, *Radio Sci., 19*, 1475–1484, 1984.

Larsen, M. F., and J. Röttger, VHF and UHF Doppler radars as tools for synoptic research, *Bull. Am. Meteorol. Soc., 63*, 996–1008, 1982.

S. Fukao and I. Kimura, Department of Electrical Engineering, Kyoto University, Yoshida, Kyoto 606, Japan.

H. Hojo, NTT Electrical Communications Laboratories, Yokosuka, Kanagawa 238, Japan.

S. Kato and T. Sato, Radio Atmospheric Science Center, Kyoto University, Uji, Kyoto 611, Japan.